Available online at www.sciencedirect.com

ScienceDirect

Polymer 47 (2006) 7747–7759

polymer

www.elsevier.com/locate/polymer

Confinement, composition, and spin-coating effects on the glass transition and stress relaxation of thin films of polystyrene and styrene-containing random copolymers: Sensing by intrinsic fluorescence

Manish K. Mundra [a], Christopher J. Ellison [b], Ross E. Behling [b], John M. Torkelson [a,b,*]

[a] Department of Materials Science and Engineering, Northwestern University, Evanston, IL 60208-3120, USA
[b] Department of Chemical and Biological Engineering, Northwestern University, Evanston, IL 60208-3120, USA

Received 30 June 2006; received in revised form 25 August 2006; accepted 30 August 2006

Abstract

The glass transition temperatures (T_gs) of polystyrene (PS) and styrene/methyl methacrylate (S/MMA) random copolymer films are characterized by intrinsic fluorescence, i.e., monomer fluorescence from an excited-state phenyl ring and excimer fluorescence from an excited-state dimer of two phenyl rings. The T_g is determined from the intersection of the rubbery- and glassy-state temperature dependences of the integrated fluorescence intensity measured upon cooling from an equilibrated state. With PS, the effects of nanoconfinement on T_g and the transition strength agree with results from studies using probe fluorescence and ellipsometry. The T_g-nanoconfinement effect is "tuned" by copolymer composition. As S-content is reduced from 100 mol% to 22 mol%, the confinement effect changes from a reduction to an enhancement of T_g relative to bulk T_g. Intrinsic fluorescence is also a powerful tool for characterizing relaxation of residual stresses. Stresses induced by spin coating affect local conformations, which in turn affect excimer and monomer fluorescence and thereby integrated intensity. The heating protocol needed to achieve apparently equilibrated local conformations is determined by equivalence in the integrated intensities obtained upon heating and subsequent cooling. While partial stress relaxation occurs upon heating in the glassy state, full relaxation of local conformations requires that a film be heated above T_g for times that are long relative to the average cooperative segmental relaxation time. For example, in thin and ultrathin films, equilibration is achieved by heating slowly (~1 K/min) to 15–20 K above T_g. Dilute solution fluorescence of PS and S/MMA copolymers is also characterized and compared to reports in the literature.

Keywords: Glass transition; Thin film; Copolymer

1. Introduction

Nanoscale confinement of polymers can lead to significant deviations from bulk polymer behavior, including those related to crystallization [1–4], physical cross-linking in associative polymers [5], thermal expansion coefficients [6–12], the glass transition temperature (T_g) [10–34], and physical aging [33–35]. Some of the earliest as well as very recent studies on thermal expansion coefficient and T_g behavior in nanoconfined polymer films have indicated that there can be significant effects associated with the process and thermal history of the films [6,8,9,11,22]. Several studies have specifically suggested that some of the unusual or anomalous T_g-behavior observed in ultrathin films may be associated with stresses that are built-in during the spin-coating or spin-casting process and remain unrelaxed during the T_g measurement [12,35,36]. While it has been appreciated for at least twenty-five years that polymer film formation by spin coating and even the much milder solvent-casting process can lead to orientation and non-equilibrium conformations of polymer chains and thereby residual stress effects [36–41], there has been relatively little direct comparison [8,9] of how the thermal

---

* Corresponding author. Department of Chemical and Biological Engineering, Northwestern University, Evanston, IL 60208-3120, USA.
E-mail address: j-torkelson@northwestern.edu (J.M. Torkelson).

0032-3861/$ - see front matter © 2006 Published by Elsevier Ltd.
doi:10.1016/j.polymer.2006.08.064

history of spin-coated polymer films leads to relaxation of residual stresses in polymer films and whether the apparent T_g is affected by unrelaxed residual stresses.

A potentially powerful manner with which to obtain a qualitative measure of the residual stresses in spin-coated films of polystyrene (PS) in combination with T_g values in polymer films is intrinsic fluorescence. Intrinsic fluorescence of PS consists of both monomer and excimer fluorescence, the former due to emission from a single excited-state phenyl ring and the latter due to emission from an excited-state dimer consisting of two phenyl rings in a parallel, sandwich-like conformation with an inter-ring separation distance of 3–4 Å [42]. Intrinsic fluorescence of PS and other polymers has been shown to be highly sensitive to issues ranging from local polymer conformational populations in solution and phase behavior in solvents and polymer blends to local microenvironments in bulk homopolymers [43–58]. In particular, excimer formation in PS solutions and blends is almost exclusively associated with *trans–trans* conformations in *meso* dyads along the PS chain [58,59], i.e., an increase in *trans* conformations along the local isotactic regions of a PS chain will result in an increase in intramolecular excimer fluorescence.

In 1975, Frank [60] reported that excimer fluorescence of a guest aromatic vinyl polymer, poly(2-vinylnaphthalene), dissolved in a polymer host can be used to monitor the relaxation of the non-equilibrium chain conformation distribution of the guest polymer at temperatures near the T_g of the host polymer. Later, in 1989 Frank and co-workers [61] demonstrated that the ratio of excimer fluorescence intensity to monomer fluorescence intensity, I_e/I_m, in spin-cast PS films increased with increasing spin speed (leading to decreasing thickness) and thereby radial stress. The elevated I_e/I_m values obtained in spin-cast films were qualitatively consistent with the results of a study [62] showing that uniaxial alignment of PS films leads to an increase in I_e/I_m values. It was rationalized that chain orientation via spin casting can lead to an increase in the concentration of *trans* conformations along the chains (associated with intramolecular excimer-forming sites), the concentration of intermolecular excimer-forming sites, and a higher rate of energy migration to excimer-forming sites. (It should be noted that the use of intrinsic fluorescence to monitor relaxation of residual stress associated with the processing of polymer films is fundamentally different from studies employing extrinsic probe or label fluorescence to monitor structural relaxation or physical aging in glassy polymer films [22,33,34,63–66].)

Several years ago, our group demonstrated that the temperature dependence of the intrinsic fluorescence of a 12-μm-thick PS film may be used to determine T_g [23]. At that time, we did not obtain T_g values for ultrathin PS films (≤100 nm) using intrinsic fluorescence due to a low signal-to-noise ratio and instead used probe or label fluorescence (pyrenyl dyes or molecular "rotor" dyes) for T_g measurements [22–26,33,34]. With improved instrumentation and experimental technique, we now obtain high signal-to-noise ratios for intrinsic fluorescence measurements of thin and ultrathin films of PS and styrene (S)/methyl methacrylate (MMA) random copolymers. We show that intrinsic fluorescence from thin and ultrathin films of PS and S/MMA random copolymers can be used to characterize both the T_g (as a function of copolymer composition and process conditions) and the relative state of relaxation of the residual stresses. In order to demonstrate that the fluorescence response of the copolymers is consistent with the results in the literature and to assist the reader in understanding the intrinsic fluorescence of PS and S/MMA random copolymers, we also characterize the fluorescence of our copolymers in dilute solution and compare with studies by David et al. [67] and Reid and Soutar [68].

2. Experimental

2.1. Copolymer synthesis and characterization

Polystyrene and S/MMA random copolymers were synthesized by bulk free radical polymerization at 343 K using benzoyl peroxide (Aldrich, 97%) as initiator. Styrene and methyl methacrylate (Aldrich) were deinhibited with inhibitor remover (Aldrich) and dried over CaH_2. Copolymer composition was controlled by varying the comonomer content used in the copolymerizations; fractional conversions were held to less than 10% to avoid composition drift. Resulting copolymers were purified by dissolution in toluene (Fisher, 99.9%) and precipitation in methanol (Fisher, 99.9%) at least five times to remove residual monomer and initiator. Samples were dried in a vacuum oven at ~393 K for several days prior to use.

The styrene mole fraction (F_s) of each copolymer was measured via ^{1}H NMR (Varian Inova 500 MHz spectrometer) spectroscopy with $CDCl_3$ as solvent and was in good agreement with expectations based on reactivity ratios for the S/MMA system [69]. Number average molecular weights of PS and all copolymers exceeded 100,000 g/mol (gel permeation chromatography relative to PS standards in tetrahydrofuran (THF)). The bulk T_gs of PS and the copolymers were measured by differential scanning calorimetry (DSC) using a Mettler-Toledo DSC822e at a 10 K/min heating rate on the second heating cycle after quenching from elevated temperature at a rate of 40 K/min. Table 1 provides details on PS and copolymer characterization.

Table 1
Characterization of PS and S/MMA copolymers used in this study

F_s	M_S	M_{MMA}	f_{SS}	N_S	$f_{SS}N_S$	T_g (onset), DSC	T_g, Fluorescence
1.000	1.000	0.000	1.000	–	–	378 K	378 K
0.782	0.865	0.135	0.597	4.34	2.591	376 K	379 K
0.652	0.730	0.270	0.372	2.41	0.895	377 K	377 K
0.581	0.637	0.363	0.266	1.91	0.508	378 K	377 K
0.390	0.343	0.657	0.073	1.27	0.093	376 K	377 K
0.215	0.124	0.876	0.027	1.07	0.029	379 K	377 K
0.088	0.025	0.975	0.013[a]	1.01	0.013	378 K	378 K

F_s is the cumulative S mol fraction in the copolymers; M_S and M_{MMA} are the mol fractions of S and MMA in the monomer mix used to make the copolymers; f_{SS} and N_S are the S–S dyad fraction and number average sequence length of S units in the copolymers, respectively. Also provided are the bulk T_g values determined by DSC and fluorescence.

[a] Denotes fraction calculated from reactivity ratios.

2.2. Solution studies

Dilute copolymer solutions were made at equal styrene repeat unit content (equivalent to 0.50 g/L PS) in THF (Aldrich, spectrophotometric grade, inhibitor free). Air-equilibrated, solution fluorescence was measured at room temperature (∼295 K) in a standard 1-cm-path-length quartz cuvette using a Photon Technologies Incorporated (PTI) QM-2001 SE fluorimeter employing a right-angle geometry, with 1 mm excitation and emission slits (band pass = 1.8 nm). Excitation was done at 260 nm, and emission was measured from 265 nm to 415 nm.

2.3. Film studies

Relatively thick films (∼5 μm) were prepared by solution casting of concentrated solutions of PS or copolymers dissolved in THF onto high-purity fused quartz slides. The slides were initially washed with a 10% sodium hydroxide/70% ethanol/20% water solution and then solvent washed. These thick films were dried for 24 h in a Petri dish followed by vacuum drying at room temperature for 24 h and then at 383 K for 36 h. The slow drying process was used to prevent bubble or crack formation. Films that developed bubbles or cracks were discarded. Thin and ultrathin films were prepared by spin coating of dilute PS or copolymer solutions in THF of various concentrations at speeds of 500–4000 rpm for 60 s, yielding film thicknesses ranging from 20 nm to 1000 nm [70,71]. In those cases in which films were used for T_g measurements only, they were then annealed in a vacuum oven for 24 h at 383 K. Films that were used for stress relaxation measurements experienced no annealing prior to measurement. Film thickness was measured with a Tencor P10 profilometer (calibration was verified by using a 14-nm step height standard from VLSI standards) by taking an average of at least 10 measurements close to the center of the film where fluorescence was measured.

A Spex Fluorolog-2DMIB fluorimeter was used to measure fluorescence of films with thickness exceeding 2000 nm. Measurements employed a front-face geometry with 2.5 mm excitation and emission slits (band pass = 4.5 nm). For thin and ultrathin films, fluorescence was measured using a PTI QM-2001 SE fluorimeter using a front-face geometry with 1 mm excitation and emission slits (band pass = 1.8 nm). As the PTI fluorimeter has greater excitation intensity than the Spex fluorimeter, the smaller slit size was used with the PTI instrument to prevent films from photobleaching at high temperature. Film temperature was controlled using a microprocessor controller (Minco Products) with a Kapton ribbon heater attached to a flat aluminum plate with a hole in the center to prevent scattering or fluorescence from the heater itself. For intrinsic fluorescence, excitation was done at 260 nm, and the emission spectrum was measured from 270 nm to 410 nm. For pyrene-doped samples, excitation was done at 322 nm, and the emission spectrum was measured from 360 nm to 460 nm. Pyrene (Aldrich, 99+% purity) was used as received. Unless otherwise specified, fluorescence spectra used to measure T_g were recorded upon cooling after having annealed samples at $\sim T_g + 40$ K for 15–60 min. For further information on measurement of T_gs by fluorescence, see Refs. [22–26].

An M-2000D™ spectroscopic ellipsometer (J. A. Woollam Co., Inc.) with an integrated programmable heating source (Instec) was used for measurements characterizing film thickness as a function of temperature above and below T_g with several heating and cooling cycles. Several heating and cooling cycles were employed with each measurement.

3. Results and discussion

3.1. Solution studies

Fig. 1 illustrates how fluorescence intensity and spectral shape are functions of S composition in dilute solutions of S/MMA copolymers and PS. Fig. 1a compares the spectrum of PS with those of 58/42 mol% and 22/78 mol% S/MMA random copolymers. For PS, a maximum intensity is observed at ∼328 nm, indicative of excimer fluorescence, with a second, lesser peak at ∼285 nm indicative of monomer fluorescence (with some contribution from excimer fluorescence). With decreasing S-content in the copolymers, there is a reduction in excimer fluorescence and a major increase in monomer fluorescence. In addition, an isobestic or isoemissive point (point of common intensity) is observed at ∼320 nm. This point is characteristic of the fact that the fluorescence in these systems, which contain equivalent concentrations of S repeat units, is associated with only two potentially interconvertible species [72], excited-state monomer and excimer.

Fig. 1b compares the spectral shapes of PS with 78/22 mol% S/MMA copolymer and of 22/78 mol% S/MMA copolymer with 9/91 mol% S/MMA copolymer. In the case of PS and the high S-content copolymers, the spectral shapes are identical at wavelengths of 335 nm and greater, indicating that, within error, all fluorescence in this range is due to excimer fluorescence. However, PS and the high S-content copolymers differ greatly in spectral shapes at lower wavelengths due to the increasing amount of monomer fluorescence with decreasing S-content. In the case of the two lowest S-content copolymers, the spectral shapes are nearly identical and, within error, indicate a nearly complete absence of excimer fluorescence. The details of the fluorescence spectra presented in Fig. 1 are in accord with previous studies of the fluorescence of dilute solutions of PS and random S/MMA copolymers [43–45,47–50,67,68,73].

The results in Fig. 1 indicate that characteristic values of I_e/I_m may be obtained from measurements of fluorescence intensities at two wavelengths. A characteristic value of I_e is obtained by measuring intensity at high wavelength where monomer fluorescence is absent, here the intensity at 360 nm is taken to be characteristic of I_e. A characteristic value of I_m is obtained by measuring intensity at low wavelength, 280 nm in the present study, and correcting for the contribution made by excimer fluorescence at that wavelength. We have followed the approach used earlier by David et al. for

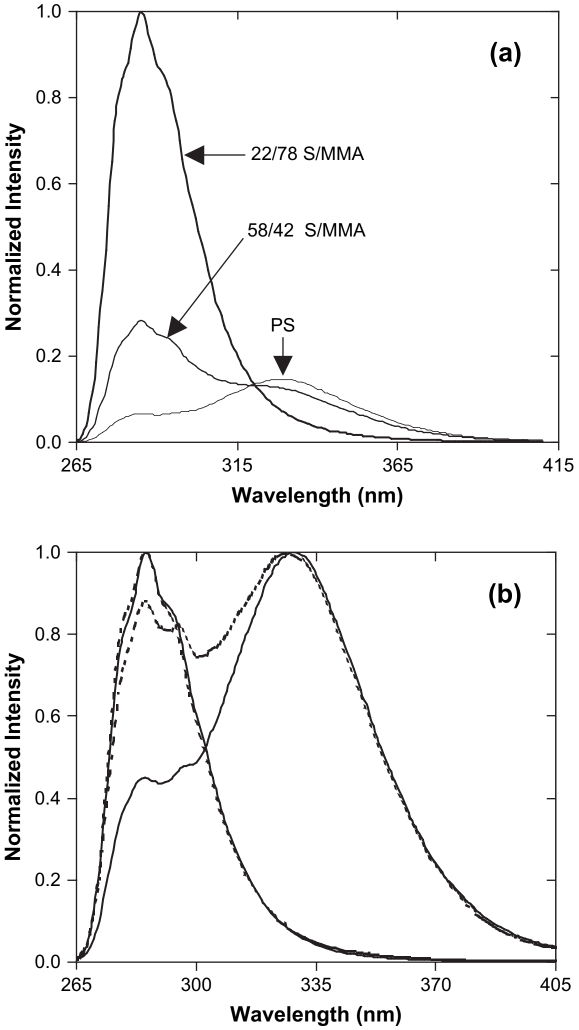

Fig. 1. (a) Fluorescence emission spectra of dilute solutions of PS and S/MMA copolymers in THF as a function of S mol fraction. Solutions contain an equal S repeat unit concentration of 0.50 g/L. Spectra are normalized to unity at the peak intensity of the 22/78 mol% S/MMA copolymer. (b) Fluorescence emission spectra of dilute solutions of PS and S/MMA copolymers in THF. Spectra with peak intensities at ~328 nm are for PS (bold line) and 78/22 mol% S/MMA copolymer (dashed line). Spectra with peaks at ~285 nm are for 9/91 mol% S/MMA (bold line) and 22/78 mol% S/MMA (dashed line). Solutions contain an equal S repeat unit concentration of 0.50 g/L. Spectra are normalized to unity by their individual peak intensity.

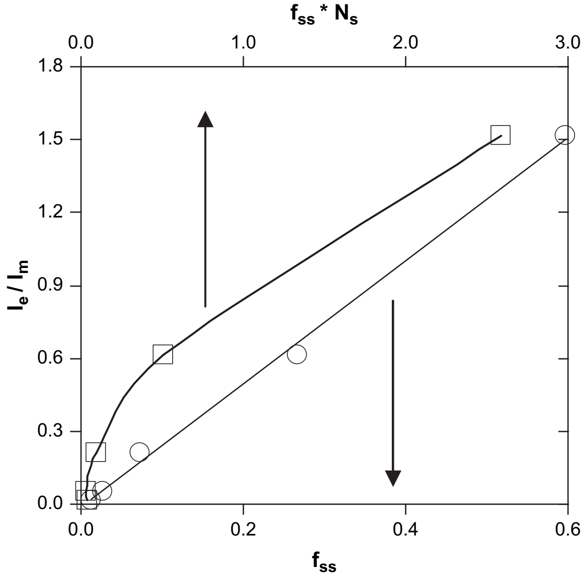

Fig. 2. Excimer to monomer fluorescence intensity ratio of dilute solutions of S/MMA random copolymers as a function of the S–S dyad fraction (f_{SS}) and the product of the S–S dyad fraction and number average sequence length of styrene units ($f_{SS}N_S$) in the copolymers.

making this correction. See Ref. [67] for details. (In the discussion below related to Fig. 2, we note that the same conclusions are reached whether I_m is taken to be the uncorrected intensity at 280 nm or a correction is made to account for the contribution of excimer fluorescence at 280 nm.)

Two pictures have been presented in the research literature regarding how I_e/I_m values obtained in dilute solution fluorescence depend on the composition of S-containing copolymers. David et al. [67] indicated that excimer fluorescence is a direct result of bond rotations that lead to excimer when an excited-state monomer forms a parallel, sandwich-like conformation with a second monomer (phenyl ring) with the requisite inter-phenyl-ring distance to yield an excited-state dimer. In this picture, I_e/I_m is a linear function of the S–S dyad fraction, f_{SS}, in the copolymer. Reid and Soutar [68] included the possibility of excimer formation occurring by energy migration of an exciton along neighboring phenyl rings on the chain backbone to an excimer-forming site. In this picture, I_e/I_m is a linear function of the product of the number average sequence length of S units in the copolymer, N_S, and f_{SS}. David et al. [67] provided data on S/MMA copolymers consistent with the notion that I_e/I_m is proportional to f_{SS} while Reid and Soutar [68] provided data consistent with the notion that I_e/I_m is proportional to N_Sf_{SS}.

In Fig. 2, we provide plots of the values of I_e/I_m from our dilute solutions of S/MMA copolymer as functions of f_{SS} and N_Sf_{SS}. (The intensity ratios shown in Fig. 2 were calculated after subtracting out the contribution of excimer fluorescence to the intensity measured at 280 nm. However, the same conclusion is reached even if the intensity ratio employed the intensity at 280 nm without correction for excimer contribution.) In order to draw an exact comparison of our results with the differing conclusions reached by David et al. [67] and Reid and Soutar [68], we have calculated the values of f_{SS} and N_S in exactly the same way they did, using the method of Harwood and Ritchey and assuming a terminal model for copolymerization [74]. (While the terminal model does not perfectly describe S/MMA copolymerization, the direct comparison it allows with previous research results makes this approach useful in the context of our study.) Fig. 2 indicates that our data are reasonably approximated by a linear function of f_{SS} and are not well represented by a linear function of N_Sf_{SS}. Thus, our results are in accord with the picture of David et al. [67] which in turn indicates that any contribution of energy migration to excimer formation in dilute solutions of S-containing copolymers is small. This is consistent with previous research that concluded that energy migration has a negligible effect on fluorescence of dilute PS solutions [75]. This is in contrast to the significant evidence [44,57] for the impact of energy migration in the fluorescence behavior of neat PS and blends containing PS; energy migration may include interpolymer effects in these systems that are dense with phenyl rings.

3.2. T_g-confinement effects as a function of S/MMA copolymer composition: Thin film measurements via intrinsic fluorescence.

Fig. 3 compares the intrinsic, room-temperature fluorescence emission spectra of neat, bulk films of PS and two S/MMA copolymers; each spectrum has been normalized to unity at the peak intensity. The neat, bulk PS film exhibits mostly excimer fluorescence and little monomer fluorescence, much less than that observed in dilute solution relative to excimer fluorescence (Fig. 1). A significant shift from excimer to monomer fluorescence is observed with decreasing styrene content in the copolymers. However, as with the neat PS, I_e/I_m is significantly greater in a copolymer film of given composition than in a dilute copolymer solution of the same composition. This effect may be due to several factors [58]: different conformational states in the bulk film as compared to dilute solution favoring intramolecular excimer formation; interpolymer excimer formation in the bulk film; and an enhancement, relative to dilute solution, in the migration of the excited-state energy to an excimer-forming site in the bulk film.

Previous research [23] has shown that the T_g value of bulk, neat PS can be measured by plotting intrinsic fluorescence intensity at a given wavelength as a function of temperature over a range of at least 60–70 K roughly centered at T_g. The T_g is determined via the intersection of the linear temperature dependences of intensity deep in the rubbery and glassy states. In the results described below, we employ plots of integrated intensity (integrated across the fluorescence spectrum) as a function of temperature. As reported recently in an extrinsic fluorescence study [26], this approach minimizes errors, leading to more precise T_g determinations. (Within experimental error, identical T_g determinations are made when fluorescence is monitored as a function of temperature over a range of 100–110 K or a range of 60–70 K around T_g.)

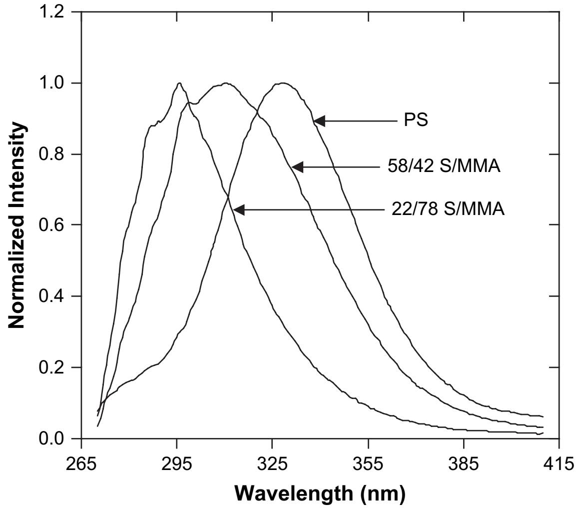

Fig. 3. Intrinsic fluorescence emission spectra for bulk films (4–5 μm thick) of PS and 58/42 mol% S/MMA and 22/78 S/MMA random copolymers at room temperature. Intensity is normalized to unity at the peak intensity of each film.

Fig. 4 shows T_g determinations for films of PS and selected S/MMA copolymers from the temperature dependence of integrated fluorescence intensity. The integrated intensity, which is proportional to the fluorescence quantum yield, is expected to decrease with increasing temperature because of an enhancement of non-radiative decay rates with increasing thermal energy. However, the change in the temperature dependence at T_g is a manifestation of the change in the temperature dependence of polymer density which also affects non-radiative decay processes [24]. Several points are noteworthy from Fig. 4. In each case, there is a reduction in the *strength* of the glass transition (defined by the change between the rubbery- and glassy-state temperature dependences of intensity) in the ultrathin films relative to the thin films, a result that is consistent with previous determinations of T_g in PS films using extrinsic pyrene probe fluorescence [24] and ellipsometry [10]. (Fig. 4c and e provide rescaled plots of data shown in Fig. 4b and d for systems in which the T_g strength is particularly weak; these rescaled plots show that precise T_g values can nevertheless be obtained in such cases with fluorescence data of sufficient quality.) Second, the overall change in integrated intensity with temperature is much smaller in ultrathin films, a result also found using extrinsic pyrene fluorescence to determine T_g in PS and several other styrenic-based homopolymers [26]. Finally, in the case of low S mol% copolymers, e.g., 22/78 mol% and 9/91 mol% S/MMA, the temperature dependence of intensity in the glassy state is greater than that in the rubbery state, the opposite of what is observed in PS films or copolymers with 39 mol% or greater S-content. (These results imply that there must be a copolymer composition with S-content greater than 22 mol% and less than 39 mol% that yields essentially no sensitivity of intrinsic fluorescence to T_g. In that case, a fluorescence probe such as pyrene could be added at trace levels to the copolymer film to determine T_g via extrinsic fluorescence [22–26].)

In our previous studies in which T_gs of PS and poly(methyl methacrylate) were measured via pyrene probe or label fluorescence [22–26,33,34], a greater temperature dependence of intensity was always observed in the rubbery state, in accord with the notion that a significant portion of the temperature dependence of fluorescence of pyrenyl dyes in glass-forming polymers reflects local density effects, i.e., a slightly denser local environment near a pyrene dye accommodates less non-radiative decay of the excited state leading to higher intensity. As the thermal expansion coefficient is greater in the rubbery state than in the glassy state, this impact of density should yield a stronger temperature dependence of intensity in the rubbery state, consistent with the results observed in the higher S-content copolymers (where much of the fluorescence is due to excimers). Obviously, this explanation does not hold for the low S-content copolymers (where nearly all fluorescence is due to emission from single excited-state phenyl rings rather than excimers).

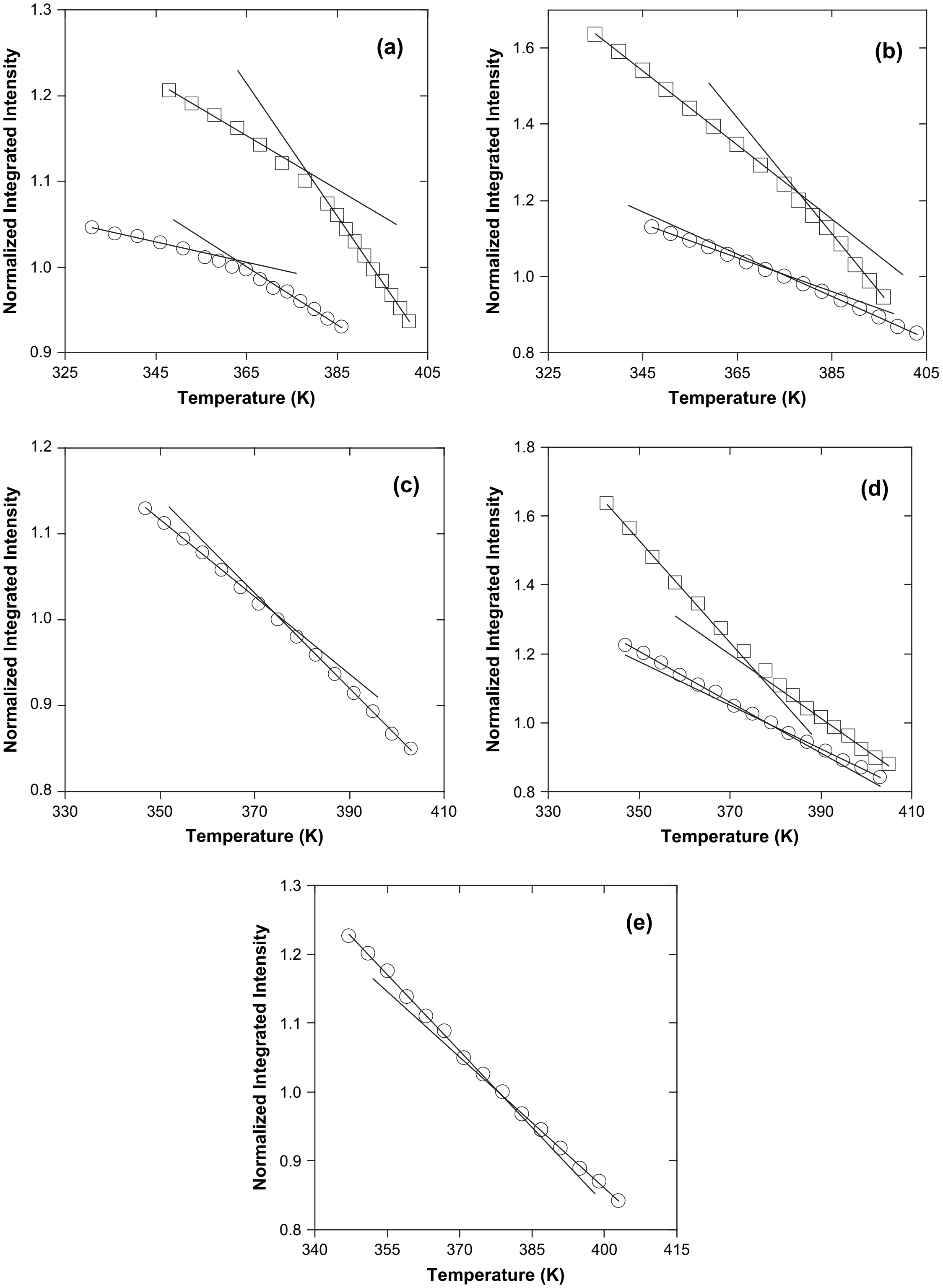

Fig. 4. (a) Temperature dependence of the integrated intrinsic fluorescence intensity for 4570-nm thick (□) and 22-nm thick (○) PS films. (The integrated intensity is normalized to unity at the respective T_g of each film and arbitrarily shifted.) (b) Temperature dependence of the integrated intrinsic fluorescence intensity of the 39/61 mol% S/MMA random copolymer in 4690-nm thick (□) and 21-nm thick (○) films. (The integrated intensity is normalized to unity at the respective T_g of each film and arbitrarily shifted.) (c) Expanded plot of the data shown in (b) for the 21-nm thick film (○). (The integrated intensity is normalized to unity at T_g.) (d) Temperature dependence of the integrated intrinsic fluorescence intensity of the 22/78 mol% S/MMA random copolymer in 230-nm thick (□) and 90-nm thick (○) films. (The integrated intensity is normalized to unity at the respective T_g of each film and arbitrarily shifted.) (e) Expanded plot of the data shown in (d) for the 90-nm thick film (○). (The integrated intensity is normalized to unity at T_g.)

It is interesting to note that previous research has shown that in certain cases the temperature dependence of the fluorescence of molecular "rotor" or twisted intramolecular charge transfer (TICT) probes or labels can be used to obtain T_g values in bulk [76] and ultrathin [32,33,77,78] polymer films and that there is a stronger temperature dependence of intensity in the glassy state than in the rubbery state. Obviously, the phenyl rings in the low S-content copolymers under study here are not of the classic "rotor" or TICT type, and further study will be needed to explain the exact origin of the temperature dependence of fluorescence intensity observed in films of such copolymers. Nevertheless, intrinsic fluorescence measurements of bulk films yield T_gs in excellent agreement with those obtained by DSC (see Table 1).

Fig. 5 shows the thickness dependence of $T_g - T_{g,bulk}$ as a function of S-content for various S/MMA copolymer compositions; in all cases, T_g data were obtained using the method shown in Fig. 4. The data in Fig. 5 indicate that the T_g-nanoconfinement effect may be "tuned" via copolymer composition. The intrinsic fluorescence of PS shows a thickness dependence of $T_g - T_{g,bulk}$ similar to that obtained with extrinsic fluorescence of pyrene doped into or covalently attached to neat PS. (The T_g data obtained from pyrene dopant or label fluorescence [24] were previously shown to be in good agreement with T_g data obtained by Keddie et al. [13] using ellipsometry.) As the styrene content is reduced from 100 mol% to 22 mol%, the effect of confinement on T_g changes from a reduction to an enhancement of T_g relative to $T_{g,bulk}$. This "tunability" of the T_g-confinement effect with copolymer composition as observed by intrinsic fluorescence is in good agreement with results of a recent ellipsometry study by Park et al. [27]. In addition to PS and PMMA films, Park et al. employed two MMA-rich copolymers, which yielded smaller reductions in T_g with decreasing thickness than those observed for neat PS films. The effect of copolymer composition can be explained by the difference in the polymer–substrate interaction. Styrene repeat units exhibit no attractive interaction with the substrate; thus, supported PS films undergo a T_g reduction with confinement due to the T_g reduction originating at the free surface (polymer–air interface) of the film [24]. In contrast, MMA repeat units can undergo hydrogen bonding with the silanol units naturally present on the substrate (quartz) surface, which reduces the level of cooperative segmental mobility and thereby leads to an enhancement in T_g of PMMA films with confinement.

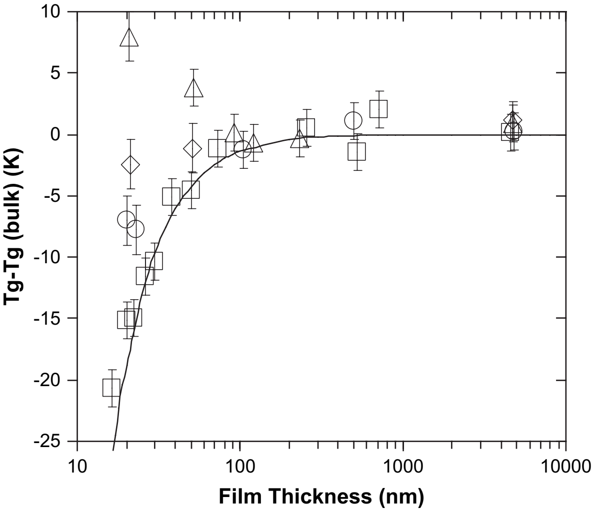

Fig. 5. Film thickness dependence of $T_g - T_{g,bulk}$ as measured by intrinsic fluorescence: PS (□), 58/42 mol% S/MMA random copolymer (○), 39/61 mol% S/MMA random copolymer (◇), and 22/78 mol% S/MMA random copolymer (△). The curve represents a fit to PS film data from Ref. [26] measured using extrinsic probe fluorescence; the fit employs the empirical relation originally proposed by Keddie et al. [13], yielding the parameter values $A = 3.2$ nm and $\delta = 1.63$ (reported previously in Ref. [26]).

It is noteworthy that the tunability of the T_g-confinement effect in supported S/MMA copolymer films yields an apparent near invariance of T_g with film thickness in the case of the 39/61 mol% S/MMA copolymer. This may be understood to arise from a balancing of the effects associated with the free surface leading to a reduction in T_g with confinement and attractive polymer–substrate interactions leading to an enhancement of T_g. Thus, the perturbations to T_g caused by free surfaces and polymer–substrate interfacial interactions remain present in this system even though the cumulative effect *across* a nanoconfined film yields an average measured T_g value very close to that of a bulk film.

3.3. Stress relaxation effects in thin and ultrathin films measured by intrinsic fluorescence

Here we employ fluorescence spectroscopy of PS and styrene-containing copolymer films to investigate stress relaxation in spin-coated thin and ultrathin films that are not annealed above T_g prior to measurement. The experimental protocol for this section of our study involves heating spin-coated, unannealed samples by 5 K increments, remaining at the temperature for 5 min, measuring fluorescence, and then heating by 5 K, etc. When a temperature is reached that is well above T_g, the sample is then cooled by 5 K, temperature is maintained for 5 min, fluorescence is measured, and then the sample is cooled by 5 K, etc.

Fig. 6a shows the temperature dependence during heating and cooling of the integrated intrinsic fluorescence intensity for a 260-nm thick PS film. There is a major difference in the intrinsic fluorescence intensity during heating and cooling cycles for temperatures less than ~390 K; at temperatures greater than ~390 K, the fluorescence responses during heating and cooling are the same within experimental error.

These results indicate that stresses induced during spin coating affect the distribution of local conformational populations in the PS film, which in turn affect the levels of excimer and monomer fluorescence. It must be noted that excimer is often formed from excited-state monomer and results in the loss of monomer fluorescence. This fact in combination with the fact that excimer fluorescence has a low quantum yield means that integrated fluorescence intensity is reduced when there is more excimer formation. In Fig. 6a, there is a sharp increase in intensity with increasing temperature as the unannealed film is heated from 348 K to 368 K. (Similar, although

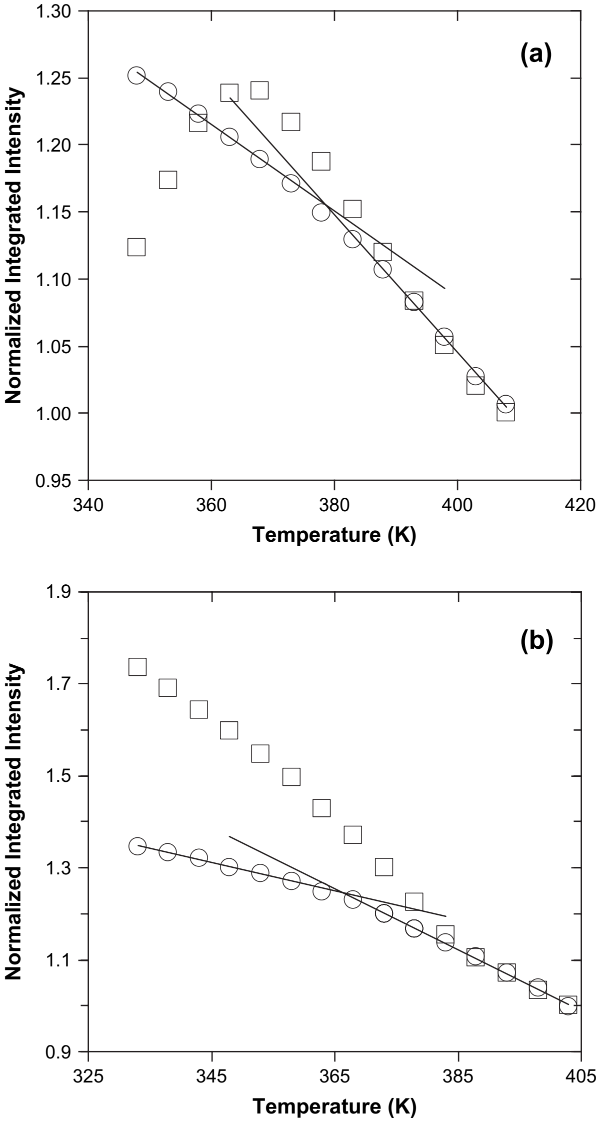

Fig. 6. (a) Temperature dependence of the integrated intrinsic fluorescence intensity of a 260-nm thick PS film during heating (□) and cooling (○) cycles. (The integrated intensities are normalized to unity by the intensity at 408 K measured during heating.) (b) Temperature dependence of the integrated intrinsic fluorescence intensity of a 26-nm thick PS film during heating (□) and cooling (○) cycles. (The integrated intensities are normalized to unity by the intensity at 403 K measured during heating.)

not identical, results to those shown in Fig. 6a are obtained during the first heating cycle with other unannealed PS films of identical thickness but made with different spin-coating rotational speeds, ranging from 400 rpm to 3600 rpm, and different solution concentrations. The small differences in the fluorescence exhibited among these films during the first heating cycle may be a manifestation of small differences in residual stresses caused by the use of different spin speeds and solution concentrations.) The temperature dependence of intensity is the opposite in well-annealed PS films (see Fig. 4a). This means that the increase in intensity observed upon heating to 368 K in Fig. 6a is due to a change in local conformational population that disfavors excimer fluorescence. In other words, the stresses associated with spin coating of this film result in local conformations favoring excimer formation (*trans* conformations) beyond that present in well-equilibrated films, and annealing at temperatures significantly below T_g then leads to some stress relaxation and local conformational populations less favorable for excimers. (This behavior is consistent with that reported by Frank [60] regarding the impact of spin coating on the fluorescence of PS films.) Upon further heating, there is a decrease in intensity. The fact that the intensities upon heating and cooling match at 393 K means that during the heating cycle there is sufficient stress relaxation when the temperature reaches 393 K for the local conformational population in the PS film to be identical within error to that in films experiencing yet further annealing.

This latter point is important because while *some* stress relaxation occurs during heating in the glassy state well below T_g, the non-equilibrated local conformational populations cannot be fully relaxed by heating a few degrees above T_g for several minutes. Instead, as measured via intrinsic PS fluorescence and using the heating protocol described above, the stresses induced by spin coating are relaxed only when a temperature of 393 K is reached, 15 K above the T_g of the film. Note that an accurate T_g value can be obtained only during the cooling cycle and not during the initial heating cycle; the T_g value obtained during the cooling cycle measurement is 378 K, in good agreement with the T_g value measured by DSC for bulk PS and by intrinsic fluorescence in well-annealed PS films (see Table 1).

We note that the unusual fluorescence results exhibited during the first heating cycle in Fig. 6a cannot be explained by the presence of residual solvent in the film after spin casting; instead, it must be associated with the relaxation of non-equilibrated local conformational populations resulting from the spin coating of the film. Spectroscopic ellipsometry was used to measure film thickness as a function of repeated heating and cooling cycles for a film that was spin coated using conditions identical to those used in making the film studied in Fig. 6a. The as-spin-coated initial film had a thickness at 298 K that was 0.2% greater than the film exhibited at 298 K during all subsequent cooling cycles from temperatures well above T_g. This means that not more than ∼0.2 wt% residual THF solvent was present in the film at the beginning of the measurement shown in Fig. 6a. This trace level of residual solvent could not lead to the unusual fluorescence behavior exhibited during the first heating cycle in Fig. 6a.

Fig. 6b shows the temperature dependence of the integrated fluorescence intensity during heating and cooling of a 26-nm thick PS film. In contrast to the results in Fig. 6a, there is a sharp drop in the integrated intensity upon heating the unannealed film. The integrated intensities upon heating and cooling are identical only for temperatures greater than or equal to 383 K.

These results indicate that stress relaxation of the unannealed, ultrathin PS film occurs during heating by an increase in local conformational population favoring excimer fluorescence; hence, there is a net reduction in integrated fluorescence intensity, the exact opposite of that observed in the thicker PS film. The reason for this difference between the thin and ultrathin films is unclear. Nevertheless, the results indicate that the effect of stresses on local conformational populations may differ significantly in thin and ultrathin PS films. Notably, the ultrathin PS film exhibits identical fluorescence intensities upon heating and cooling at ∼17 K above the film T_g (T_g is ∼366 K as measured during the cooling cycle). Thus, with the given heating protocol that accounts for the different T_gs in thin and ultrathin PS films, the temperatures above T_g required to achieve stress relaxation leading to apparently equilibrated local conformational populations in thin and ultrathin spin-coated PS films are nearly identical.

Fig. 7 shows related results for heating and cooling of unannealed, thin and ultrathin PS films in which pyrene dopants are present in 0.2 wt%. The fluorescence data are the normalized integrated intensities of the pyrene dopant, which should not directly reflect local conformational populations in the PS films. In these cases, the differences observed between the fluorescence measurements obtained upon heating and cooling are much smaller than those in Fig. 6 where measurements involved intrinsic fluorescence from the PS chains themselves. While fluorescence can be a useful method to characterize relaxation of stresses in spin-coated films, Fig. 7 indicates that this approach may yield little value if the fluorescence is being obtained from probes that are not intrinsically a part of the chains themselves and do not reflect the conformational or orientation state of the polymer. However, the small difference observed between the pyrene probe fluorescence upon heating and cooling of PS films indicates that even probe fluorescence may be affected to a small yet measurable extent by unrelaxed stresses. Thus, when T_g values are determined from probe fluorescence, the data should be obtained (whenever possible) upon cooling from a temperature well above T_g.

Fig. 8 provides data similar to those in Fig. 6 except that the system is a 58/42 mol% S/MMA copolymer, where significant levels of both monomer and excimer fluorescence are present, and the film thicknesses are 500 nm (Fig. 8a) and 20 nm (Fig. 8b). In contrast to the results given in Fig. 6 for PS, with this copolymer system the temperature dependence is observed to be monotonic with temperature. However, as with Fig. 6, the intensities in the heating and cooling cycles are only matched at temperatures significantly above the T_g of each film. In the case of the 500-nm thick film, the match in intensity data occurs at ∼22 K above the film T_g while in the case of the 20-nm thick film the match in intensity occurs at ∼17 K above the film T_g. Thus, these results indicate that the stress relaxation accompanying heating of unannealed S/MMA copolymer films is similar to that accompanying heating of unannealed PS films, meaning that the attractive hydrogen bonding interactions present at the substrate in the S/MMA copolymer film have little impact in suppressing stress relaxation associated with spin coating when the films are nearly 20 K above T_g. In both the PS and 58/42 mol% S/MMA copolymer films, a heating protocol of 5 K increments every 5 min requires that the temperature reaches a value of 15–22 K above T_g for apparently full relaxation of stresses associated with non-equilibrated local conformational populations sensed by intrinsic fluorescence.

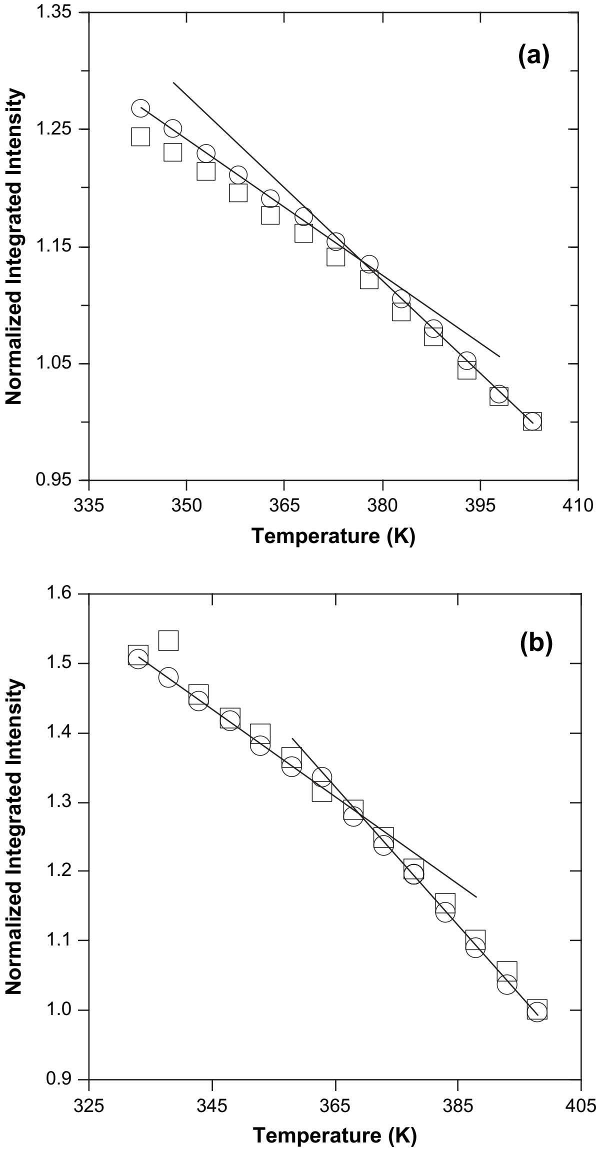

Fig. 7. (a) Temperature dependence of the integrated extrinsic fluorescence intensity an 1180-nm thick PS film doped with 0.2 wt% pyrene during heating (☐) and cooling (○) cycles. (The integrated intensities are normalized to unity by the intensity at 403 K measured during heating. (b) Temperature dependence of the extrinsic fluorescence integrated intensity of PS doped with 0.2 wt% pyrene in 35-nm thick film during heating (☐) and cooling (○) cycles. (The integrated intensities are normalized to unity by the intensity at 398 K measured during heating.

Fig. 9 demonstrates that fluorescence can provide some characterization of stress relaxation of S/MMA random copolymers even when the S-content is sufficiently low so that the excimer fluorescence is negligible. It may be possible that local conformational populations affect the rates of radiative and non-radiative decay of the excited monomer species in such copolymers, thereby accounting for the apparent sensitivity of their fluorescence intensities to stress relaxation. In particular, the data in Fig. 9 are for the 22/78 mol% S/MMA copolymer system where the fluorescence spectrum is almost exclusively due to monomer fluorescence. Nevertheless, there are major differences in the fluorescence data obtained from

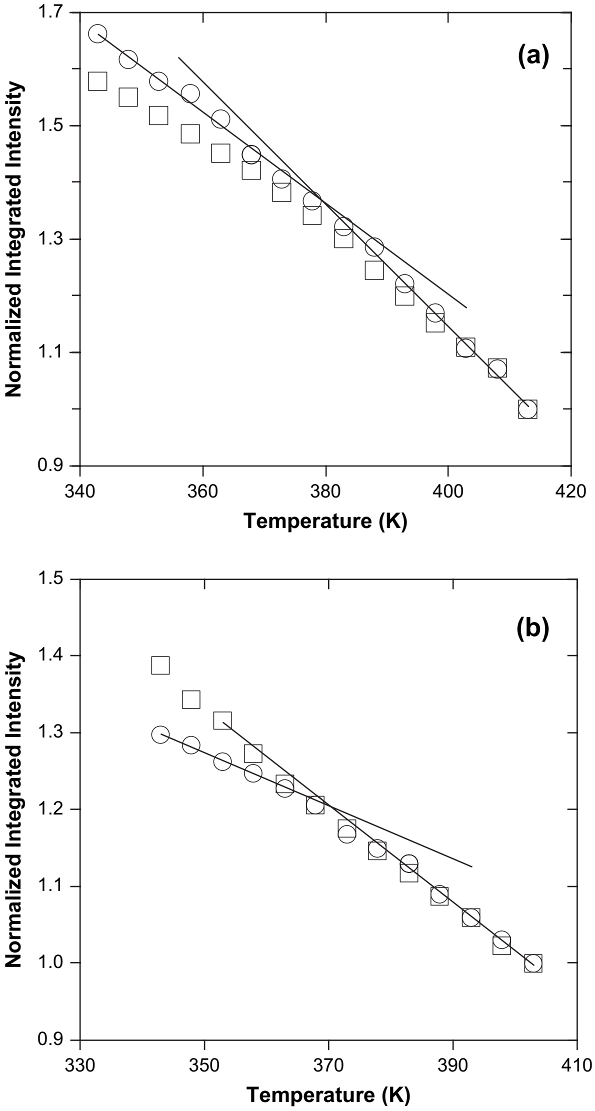

Fig. 8. (a) Temperature dependence of the integrated intrinsic fluorescence intensity of a 500-nm thick 58/42 mol% S/MMA film during heating (☐) and cooling (○) cycles. (The integrated intensities are normalized to unity by the intensity at 413 K measured during heating.) (b) Temperature dependence of the integrated intrinsic fluorescence intensity of a 20-nm thick 58/42 mol% S/MMA film during heating (☐) and cooling (○) cycles. (The integrated intensities are normalized to unity by the intensity at 403 K measured during heating.)

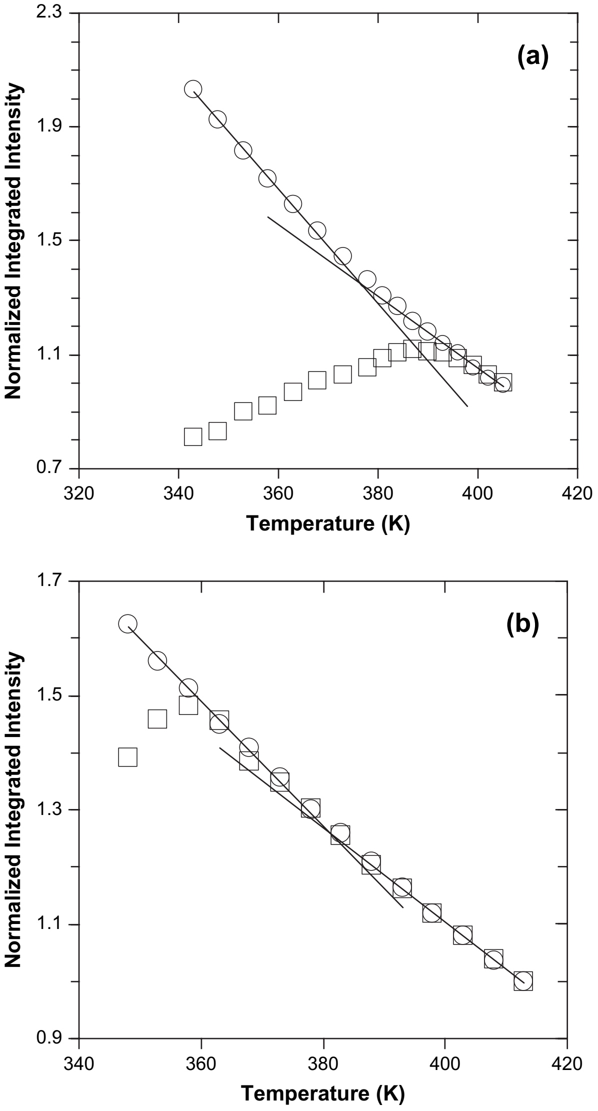

Fig. 9. (a) Temperature dependence of the integrated intrinsic fluorescence intensity of a 230-nm thick 22/78 mol% S/MMA film during heating (☐) and cooling (○) cycles. (The integrated intensities are normalized to unity by the intensity at 405 K measured during heating.) (b) Temperature dependence of the integrated intrinsic fluorescence intensity of a 50-nm thick 22/78 mol% S/MMA film during heating (☐) and cooling (○) cycles. (The integrated intensities are normalized to unity by the intensity at 413 K measured during heating.)

unannealed films of this copolymer during heating and cooling cycles. As shown in Fig. 9a, a 230-nm thick film exhibits a significant increase in intensity upon heating from ~342 K to ~390 K; with further heating, the intensity decreases. The fluorescence intensities match in the heating and cooling cycles at a temperature of 396 K (and greater), which is ~19 K above the T_g obtained from the cooling cycle. In contrast, with a 50-nm thick ultrathin film, there is a small increase in intensity upon heating from 348 K to 358 K; with further heating, the intensity decreases. The fluorescence intensities match in the heating and cooling cycles at 373 K (and greater), which is actually below the T_g of the ultrathin film. The cause of the latter outcome is uncertain. However, it is possible that better sensitivity to local conformational populations is obtained in S-containing copolymers and homopolymers that exhibit significant levels of excimer fluorescence in addition to monomer fluorescence. Further study of this point is warranted.

While these results are interesting in their own right, they also are valuable in providing guidance for the characterization of rubbery- and glassy-state behavior and T_g values of thin and ultrathin films. The results presented above indicate that significant relaxation of local conformational populations obtained in unannealed, spin-coated thin and ultrathin films of PS and S-containing copolymers can occur in the glassy state. However, with the heating protocol employed in the present study, full relaxation of the local conformational populations, as observed via intrinsic fluorescence (which is sensitive to the presence of *trans* conformations in local isotactic runs along a chain of PS or a high-to-moderate S-content copolymer), does not typically occur until the films are heated ∼15–22 K above the film T_g.

These results are in accord with the study of PS films by Frank and co-workers, [61] that found that the I_e/I_m values of high molecular weight PS films made at high spin speed (but of unreported thicknesses) relaxed toward a steady-state value over 20 min during isothermal annealing at 383 K and over much longer times at temperatures below T_g. These results are also in qualitative agreement with a portion of a recent study by Reiter and co-workers [79] who found that when 40–65 nm thick PS films (made via spin coating and never annealed above T_g prior to dewetting studies) were annealed for extended time frames in the glassy state, there were significant changes in the dewetting characteristics of these films at temperatures above T_g. A surprising feature of the study by Reiter and co-workers is that dewetting characteristics continue to be a function of annealing time below T_g even in films that experience dewetting at temperatures nearly 40 K above the bulk PS T_g. At such a high temperature, both our fluorescence data and those of Frank and co-workers [61] indicate that local conformational populations should be equilibrated quickly relative to the time scales associated with dewetting. Further investigation is needed to determine whether intrinsic fluorescence is insufficiently sensitive to some frozen-in polymer conformations that affect the high-temperature dewetting characteristics studied by Reiter and co-workers [79] or another issue beyond that associated with non-equilibrated conformations may be contributing to the effects of glassy-state annealing on dewetting of spin-coated films.

The T_g characterization obtained by intrinsic fluorescence upon cooling relaxed thin and ultrathin films of PS and S-containing copolymers agrees well with results obtained by other methods and in other studies. Hence, the film-thickness dependent T_gs that are often observed in ultrathin polymer films are not inherently a consequence of the spin-coating induced stresses accompanying the film formation. That being said, it is important to note that if the spin-coating induced stresses are not relaxed prior to measurement, as is the case of measuring film thickness upon heating of unannealed films, those stresses may affect the measurements being made because of the stress relaxation that occurs during heating. This is likely a significant contributing factor to the negative thermal expansion coefficients that have been obtained [6] upon first heating of unannealed, spin-coated polymer films. (The extent to which the effects of unrelaxed conformations contribute to cases in which negative, glassy-state thermal expansion coefficients have been reportedly observed [9,12] upon repeated heating and cooling above and below T_g in selected spin-coated ultrathin films is less clear; greater investigation is needed to determine the extent to which the heating protocols employed in such studies relax the unequilibrated conformations in those films.)

Finally, the results of our study indicate that simply heating a spin-coated polymer film to T_g and holding at temperature for a time scale equal to or several times that associated with the average cooperative segmental relaxation time, i.e., the α-relaxation time, is insufficient to relax fully the non-equilibrated conformations associated with spin-coating induced stresses [80]. Instead, as observed by intrinsic fluorescence, the full relaxation of spin-coating induced stresses in thin and ultrathin films, in which attractive polymer–substrate interactions are either present or absent, can be achieved by heating well above T_g for time scales that are long relative to average relaxation times for cooperative segmental mobility. Further study of this behavior is warranted.

4. Summary

Intrinsic fluorescence is measured in dilute solutions and thin and ultrathin films of PS and S/MMA random copolymers. Dilute solution fluorescence is characterized by a ratio of excimer to monomer fluorescence intensity. This ratio increases dramatically with increasing S-content in the copolymer and varies linearly with the S–S dyad fraction in the copolymer, in accord with a study by David et al. [67] and in disagreement with a study by Reid and Soutar [68]. This result is consistent with the notion that excimer fluorescence in dilute solution results from nearest neighbor S units with negligible impact of energy migration.

Thin and ultrathin film fluorescence is characterized via integrated fluorescence intensity. The T_g is determined from the intersection of the rubbery- and glassy-state temperature dependences of integrated intensity measured upon cooling from an equilibrated state. The T_g-nanoconfinement effect measured by intrinsic fluorescence in supported PS films agrees well with results from studies using extrinsic probe fluorescence [22,24,26] and ellipsometry [13]. The nanoconfinement effect may be tuned using copolymer composition. As S-content decreases in S/MMA copolymers, the confinement effect changes from a decrease to an increase in T_g relative to bulk T_g, with an intermediate S-content copolymer exhibiting a nearly thickness-invariant T_g. The latter effect occurs because of a balance of the effects associated with the free surface leading to a reduction in T_g with confinement and attractive polymer–substrate interactions, involving hydrogen-bonds between the hydroxyl groups on the surface of the substrate and the ester groups in the MMA repeat units, leading to an enhancement of T_g.

Intrinsic fluorescence is also a powerful tool for determining the annealing conditions needed to fully relax the unequilibrated local conformational populations that result in spin-coated PS and S/MMA copolymer films. The residual stresses induced by spin coating affect the conformational populations in the polymers; those populations affect excimer and monomer fluorescence, which in turn affect the integrated fluorescence intensity. Partial stress relaxation occurs during heating in the glassy state of thin and ultrathin films. However, with the heating protocol used here and as characterized by intrinsic fluorescence, full relaxation of the stresses induced by spin coating does not generally occur until the films, both thin and ultrathin, are heated to ∼15–20 K above T_g.

(In contrast, extrinsic probe fluorescence yields little sensitivity to residual stresses and their relaxation.) These results, coupled with the characterization of the T_g-nanoconfinement effect, indicate that many observations of modified T_g-behavior in confined films are not caused by spin-coating induced stresses. Instead, the T_g-nanoconfinement effect is present in many polymers with well-equilibrated local conformational populations.

Acknowledgments

We acknowledge the support of the NSF-MRSEC program (Grants DMR-0076097 and DMR-0520513), Northwestern University, a Henderson Dissertation-Year Fellowship (to C.J.E.), and the use of equipment in shared user facilities managed by the Materials Research Center at Northwestern University. We thank Jungki Kim for assistance with the NMR measurements of the copolymers and Connie Roth for assistance with the ellipsometry measurements.

References

[1] Frank CW, Rao V, Despotopoulou MM, Pease RFW, Hinsberg WD, Miller RD, et al. Science 1996;273:912–5.
[2] Reiter G, Castelein G, Sommer JU, Rottele A, Thurn-Albrecht T. Phys Rev Lett 2001;87:226101.
[3] Loo LY, Register RA, Ryan AJ. Phys Rev Lett 2000;84:4120–3.
[4] Jones BA, Torkelson JM. J Polym Sci Part B Polym Phys 2004;42:3470–5.
[5] Kim SD, Torkelson JM. Macromolecules 2002;35:5943–52.
[6] Orts WJ, van Zanten JH, Wu WL, Satija SK. Phys Rev Lett 1993;71:867–70.
[7] Oh WT, Ree MH. Langmuir 2004;20:6932–9.
[8] Kanaya T, Miyazaki T, Watanabe H, Nishida K, Yamana H, Tasaki S, et al. Polymer 2003;44:3769–73.
[9] Soles CL, Douglas JF, Jones RL, Wu WL. Macromolecules 2004;37:2901–8.
[10] Kawana S, Jones RAL. Phys Rev E 2001;63:021501.
[11] Beaucage G, Composto R, Stein RS. J Polym Sci Part B Polym Phys 1993;31:319–26.
[12] Mukherjee M, Bhattacharya M, Sanyal MK, Geue T, Grenzer J, Pietsch U. Phys Rev E 2002;66:061801.
[13] Keddie JL, Jones RAL, Cory RA. Europhys Lett 1994;27:59–64.
[14] van Zanten JH, Wallace WE, Wu WL. Phys Rev E 1996;53:R2053–6.
[15] Forrest JA, Dalnoki-Veress K, Stevens JR, Dutcher JR. Phys Rev Lett 1996;77:2002–5.
[16] Fryer DS, Peters RD, Kim EJ, Tomaszewski JE, de Pablo JJ, Nealey PF, et al. Macromolecules 2001;34:5627–34.
[17] Forrest JA, Dalnoki-Veress K. Adv Colloid Interface Sci 2001;94:167–96.
[18] Grohens Y, Hamon L, Reiter G, Soldera A, Holl Y. Eur Phys J E 2002;8:217–24.
[19] Pham JQ, Green PF. Macromolecules 2003;36:1665–9.
[20] Tanaka K, Arjura F, Nagamura T, Kajiyama T. Polym J 2004;36:498–501.
[21] Li L, Li B, Chen JL, Zhou DS, Xue G, Liu XN. Polymer 2004;45:2813–6.
[22] Ellison CJ, Kim SD, Hall DB, Torkelson JM. Eur Phys J E 2002;8:155–66.
[23] Ellison CJ, Torkelson JM. J Polym Sci Part B Polym Phys 2002;40:2745–58.
[24] Ellison CJ, Torkelson JM. Nat Mater 2003;2:695–700.
[25] Ellison CJ, Ruszkowski RL, Fredin NJ, Torkelson JM. Phys Rev Lett 2004;92:095702.
[26] Ellison CJ, Mundra MK, Torkelson JM. Macromolecules 2005;38:1767–78.
[27] Park CH, Kim JH, Ree M, Sohn BH, Jung JC, Zin WC. Polymer 2004;45:4507–13.
[28] Tsui OKC, Russell TP, Hawker CJ. Macromolecules 2001;34:5535–9.
[29] Blum FD, Young EN, Smith G, Sitton OC. Langmuir 2006;22:4741–4.
[30] Bernazzani P, Simon SL, Plazek DJ, Ngai KL. Eur Phys J E 2002;8:201–7.
[31] Pratt FL, Lancaster T, Brooks ML, Blundell SJ, Prokscha T, Morenzoni E, et al. Phys Rev B 2005;72:121401.
[32] Baljon ARC, Van Weert MHM, DeGraaff RB, Khare R. Macromolecules 2005;38:2391–9.
[33] Priestley RD, Broadbelt LJ, Torkelson JM. Macromolecules 2005;38:654–7.
[34] Priestley RD, Ellison CJ, Broadbelt LJ, Torkelson JM. Science 2005;309:456–9.
[35] Kawana S, Jones RAL. Eur Phys J E 2003;10:223–30.
[36] Prest WM, Luca DJ. J Appl Phys 1980;50:6067–71.
[37] Prest WM, Luca DJ. J Appl Phys 1980;51:5170–4.
[38] Cohen Y, Reich S. J Polym Sci Part B Polym Phys 1981;19:599–608.
[39] Ree M, Park YH, Kim K, Kim SI, Cho CK, Park CE. Polymer 1997;38:6333–45.
[40] Pottinger MT, Coburn JC, Edman JR. J Polym Sci Part B Polym Phys 1994;32:825–7.
[41] Lin L, Bidstrup SA. J Appl Polym Sci 1993;49:1277–89.
[42] Vala MT, Haebig J, Rice SA. J Chem Phys 1965;43:886–97.
[43] Torkelson JM, Lipsky S, Tirrell M. Macromolecules 1981;14:1601–3.
[44] Gelles R, Frank CW. Macromolecules 1982;15:1486–91.
[45] Torkelson JM, Tirrell M, Frank CW. Macromolecules 1984;17:1505–12.
[46] Major MD, Torkelson JM. Macromolecules 1986;19:2801–6.
[47] Tsai FJ, Torkelson JM. Macromolecules 1988;21:1026–33.
[48] Tsai FJ, Torkelson JM. Polymer 1988;29:1004–9.
[49] Itagaki H, Horie K, Mita I. Prog Polym Sci 1990;15:361–424.
[50] Xie R, Yang BX, Jiang BZ. Polymer 1993;34:5016–9.
[51] Clauss B, Salem DR. Macromolecules 1995;28:8328–33.
[52] Ylitalo DA, Frank CW. Polymer 1996;37:4969–78.
[53] Itagaki H, Inagaki Y, Kobayashi N. Polymer 1996;37:3553–8.
[54] Sanz A, Mendicuti F. Polymer 2002;43:6123–30.
[55] Corrales T, Peinado C, Bosch P, Catalina F. Polymer 2004;45:1545–54.
[56] Alberty KA, Hogen-Esch TE, Carlotti S. Macromol Chem Phys 2005;206:1035–42.
[57] Torkelson JM, Lipsky S, Tirrell M, Tirrell DA. Macromolecules 1983;16:326–30.
[58] Gelles R, Frank CW. Macromolecules 1982;15:747–52.
[59] Bokobza L, Jasse B, Monnerie L. Eur Polym J 1977;13:921–4.
[60] Frank CW. Macromolecules 1975;8:305–10.
[61] Kosbar LL, Kuan SWJ, Frank CW, Pease RFW. ACS Symp Ser 1989;381:95–111.
[62] Gupta MC, Gupta A. Polym Photochem 1983;3:211–9.
[63] Shmorhun M, Jamieson AM, Simha R. Polymer 1990;31:812–7.
[64] Royal JS, Torkelson JM. Macromolecules 1992;25:1705–10.
[65] Royal JS, Torkelson JM. Macromolecules 1993;26:5331–5.
[66] van den Berg O, Jager W, Cangialosi D, van Turnhout J, Verhiejen PJT, Wubbenhorst M, et al. Macromolecules 2006;39:224–31.
[67] David C, Lempereur M, Geuskens G. Eur Polym J 1973;9:1315–26.
[68] Reid RF, Soutar I. J Polym Sci Part B Polym Phys 1978;16:231–44.
[69] Brandrup J, Immergut EH, Grulke EA, editors. Polymer handbook. 4th ed. New York: Wiley; 1999.
[70] Hall DB, Underhill P, Torkelson JM. Polym Eng Sci 1998;38:2039–45.
[71] Spangler LL, Royal JS, Torkelson JM. Polym Eng Sci 1990;30:644–53.
[72] Hirayama F, Lipsky S. J Chem Phys 1969;51:1939–51.
[73] Hoyle CE, Zhao J, Orler B, Kuang W, McDonald CL. J Macromol Sci Pure Appl Chem 2001;38:527–41.

[74] Harwood HJ, Ritchey WM. J Polym Sci B Polym Lett 1964;2:601–7.
[75] Porter CFC, Phillips D. Eur Polym J 1994;30:189–96.
[76] Loutfy RO. Pure Appl Chem 1986;58:1239–48.
[77] Mundra MK, Ellison CJ, Rittigstein P, Torkelson JM. Eur Phys J Special Topics, in press.
[78] Priestley RD, Mundra MK, Rittigstein P, Broadbelt LJ, Torkelson JM. Manuscript in preparation.
[79] Reiter G, Hamieh M, Damman P, Scalvons S, Gabriele S, Vilmin T, et al. Nat Mater 2005;4:754–8.
[80] Reiter G, de Gennes PG. Eur Phys J E 2001;6:25–8.